3D Printed Active Objects based on the Promising PEDOT: PSS Resin: Investigation of their Integration inside an Electronic Circuit

International Journal of Engineering Research and Technology. ISSN 0974-3154, Volume 13, Number 3 (2020), pp. 462-469

3D Printed Active Objects based on the Promising PEDOT: PSS Resin: Investigation of their Integration inside an Electronic Circuit

Valentina Bertana[1], Giorgio Scordo[1], Matteo Manachino[1], Stefano Romano[1], Manuel Gomez Gomez[1], Simone Luigi Marasso[1,2], Sergio Ferrero[1], Matteo Cocuzza[1,2], Candido Fabrizio Pirri[1,3], Luciano Scaltrito[1]

[1] Chilab - Materials and Microsystems Laboratory, DISAT, Politecnico di Torino, via Lungo Piazza d'Armi 6, 10034 Chivasso (Turin), Italy.

[2] CNR-IMEM, Parco Area delle Scienze, 37a, 43124 Parma, Italy.

[3] Center for Sustainable Future Technologies - Istituto Italiano di Tecnologia (IIT), Via Livorno 60, 10144 Torino, Italia.

Corresponding author e-mail: valentina.bertana@polito.it

Abstract

Nowadays, the interest in the additive manufacturing (AM) field is not only from a technological point of view, but also from a materials perspective. The advantages of printing functional parts allowed the transition from AM intended as mere prototypes factory, to complete production process for small batches of highly customized devices. Especially for micrometric devices, the best solution in terms of material can be found in photo-sensitive polymers. This study was focused on finding the best way to make stereolithography (SL) printed conductive parts easily embeddable in an electronic circuit. A SL resin containing the electrically conductive polymer poly(3,4-ethylenedioxythiophene) (PEDOT) was considered for its interesting property to behave like an electrochemical transistor in proper conditions. Different standard metal plating techniques were evaluated to find out the best one for the present case study. After metallization, samples were electrically characterized to find out conductivity values. Electroplating turned out to be a valid solution, generating a metal layer on the surface without damaging the printed part and enhancing the electric contact. The reported outcomes pave the way for further studies on polymeric parts welding, which often represents a bottleneck in polymeric device integration in electronic circuits.

Keywords: Additive manufacturing; 3D conductive polymers; PEDOT:PSS; Stereolithography; Metal plating; Biomedical applications

I. INTRODUCTION

Unlike subtractive manufacturing processes, additive manufacturing (AM) can directly produce complex three-dimensional parts, with near-complete design freedom [1]. The stereolithographic technique (SL) is one of the most used AM techniques and, compared to other additive manufacturing technologies, such as fused deposition modelling - FDM - or selective laser sintering - SLS, leads to a higher accuracy of the components and degree of surface fineness, with interesting mechanical properties [2]. SL provides solid components by the selective photo-induced polymerization of a photosensitive liquid blend by means of a laser (typically in the UV range) spanning a three-dimensional CAD geometry [3].

High electrical resistivity is typical for photosensitive polymers, also known as 'resins'; when 3D printing of parts with electrical conductivity properties is needed, one or more proper conductive fillers must then be integrated in the resin. Often, at micro- and nano- scale, these fillers can be found in the literature to be metal particles [4–8], carbon nanotubes [9–11], graphene [12–14] or other electrically conductive polymers [15,16].

Once a 3D printed electrically conductive object is produced, it merely works as a technology exercise or a spare component if integration into an electronic circuit is not accomplished. Enough to say that even an electrical characterization setup requires the simplest electrical circuit to work: two wires and two probes. A good electrical connection is even more important in case of 3D printed active devices, e.g. sensors. A lot of 3D printed sensors are reported in literature, i.e. strain [17], humidity [18], gas [19], temperature [20,21], pressure [22,23] and wearable sensors [24,25], which operate according to different strategies. The common denominator between them is the difficulty to integrate those sensors in more complex circuits ensuring a good and stable ohmic contact [26]. This issue is often addressed through contact electrodes added by Ag paste spreading [20,27], thin metal layer deposition [18] or simply by crocodile clamping [19].

This work started from a previously studied polymeric resin composite [28] employed for SL: poly(ethylene glycol) diacrylate (PEGDA) was used as the photocurable matrix, while intrinsically conductive poly(3,4-ethylenedioxythiophene) (PEDOT) served to increase the resin electrical conductivity. PEDOT is a conductive polymer, which found a wide range of applications in recent literature ranging from biosensors [29–31] to energy storage [32]. Moreover, PEDOT has unique characteristics in terms of biocompatibility and interfacing with living cells [33,34].

Looking at the literature, it is easy to imagine an application for electrically conductive PEGDA:PEDOT resin. However, according to the previous considerations regarding electrical

connection, finding the right way to contact such 3D printing resin is crucial, whatever the application to be developed. First of all, it is important to consider that PEDOT works as holes transport material [35]. Therefore, it is necessary to interface a material with a higher work function (defined as the minimum required energy to extract an electron from the surface of a solid) than the PEDOT one to obtain an efficient hole injection in the semiconductor and establish an ohmic contact, maximizing the material electrical response [36]. Moreover, since metal plating on additively manufactured parts is an extra process step in the object fabrication procedure, a simple and fast metal deposition is welcome. Thus, in this paper three different metal plating techniques were compared to find the proper one for the promising PEGDA:PEDOT resin: Au sputtering, Ag paste deposition and Cu electroplating. The latter, in particular, was tested with positive results on thermoplastic printed parts [37] and on stereolithographic printed parts, but only mechanical properties were evaluated [38].

II. MATERIALS AND METHODS

Aiming to connect PEGDA:PEDOT 3D printed parts to electronic circuits elements, different metal plating techniques were investigated: one not requiring laboratory equipment, that is silver paste manual spreading. One, more accurate, requiring minimal laboratory equipment, which is copper electroplating. Finally, the more complex and expensive gold sputtering, which is one of the conventional methods to create contact pads in microelectronics. Three samples for each metal plating technique were built. Then, after metallization, samples were electrically characterized. As previously stated, the present investigation was proposed to evaluate how to properly integrate electrically conductive 3D printed parts inside a circuit. Simple parallelepiped bars, all made up by PEGDA:PEDOT resin, were chosen as tests samples.

II.I Insulating matrix

PEGDA, purchased from Sigma Aldrich, was employed as the matrix for the electrically conductive resin. When a proper photoinitiator is mixed together, PEGDA becomes UV-curable. In this case, the photoinitiator was IRGACURE 819 (used as received from Sigma Aldrich) at 1% wt. with respect to PEGDA. Mixing was carried out by a digital sonifier (Branson) at 30 kHz, operating in impulse mode (10 s ON – 5 s OFF) for 15 minutes at 30% amplitude and cooled in an ice water jacket to prevent unwanted heat-induced polymerization.

II.II Conductive polymer

Clevios PH 1000, an aqueous solution of PEDOT:PSS purchased from Heraeus, was treated before use to improve electrical conductivity, and then added to the previously prepared matrix. An aqueous solution 0.5 M of sulphuric acid (H_2SO_4 98%, purchased from Sigma Aldrich) was prepared to separate the PEDOT:PSS fraction from solvent. 1 L of acid solution was used for each 50 g of Clevios PH 1000. After 5 minutes of magnetic stirring, the solution was left to rest for 12 h. In this time, separation occurred between PEDOT, deposited on the bottom of the container, and the rest of the solution. The supernatant was manually removed and the recovered PEDOT was centrifuged at 4000 rpm for 10 minutes (OHAUS, Frontier™ 5706). Then, PEDOT was fractioned in smaller agglomerates by employing a dispersing instrument (IKA, Ultraturrax T10) for 15 minutes at velocity level 4 in a clear acid solution 0.5 M of H_2SO_4. A new centrifugation was performed in order to eliminate as much acid solution as possible. Finally, the resulting PEDOT was washed in ethanol and recovered by centrifugation.

II.III Composite resin

The insulating matrix and the conductive polymer were mixed in the proportion of 45% wt. conductive PEDOT and 55% wt. insulating PEGDA. Viscosity was adjusted by adding dimethyl sulfoxide (DMSO, Sigma Aldrich) at 5% wt. on the total weight. Magnetic stirring for 10 minutes was performed to homogenize the liquid composite resin.

II.IV 3D printing

A customized 3D stereolithography printer was used to induce the photopolymerization of the liquid composite resin for the preparation of the samples. The printer (Microla Optoelectronics s.r.l.) is able to write on a maximum area of 170 × 200 mm^2 and exploits a 405 nm wavelength laser mounted on a galvo-scanner to polymerize the blend. From a Design of Experiment (DOE) study to determinate the finest printing parameters, 15 mW nominal laser power, 2000 $mm \cdot s^{-1}$ scan velocity, 50 µm hatch spacing and 100 µm layer thickness were set as operating parameters. The sample was a 15 mm long, 10 mm wide and 1 mm thick parallelepiped. The building direction was set orthogonal to major section. Once the samples were printed, the uncured resin was gently removed with isopropyl alcohol. UV-curing post process was managed in an enclosed customized box with inert nitrogen atmosphere, through an UV lamp (LC8 Lightingcure Series, Hamamatsu) with 16 $mW \cdot cm^{-2}$ power density for 30 minutes.

II.V Samples metallization

As regards Cu electroplating, samples were immersed in an acid aqueous electrolyte solution (Ready to use TECHNI CU 2300 - Technic Inc.), made up by $CuSO_4$ dissolved salt and H_2SO_4, to perform the electrodeposition. In the experimental setup, the anode was a Cu plate, while the cathode was one of the conductive printed samples, fixed on a collector. Collector plays an important role in electrodeposition process. Good adhesion and stable electrical contact between the sample to be metal plated and the collector surface are essential to obtain a uniform deposition. In this work, two different collectors were tested: a metal plate (not Cu) and a conductive Cu tape (Copper foil tape, 3M). In the first case, an adhesive interface was needed to clamp the polymeric sample to the

metal plate. Unfortunately, the insulating adhesive layer prevented a good electrical contact. Thus, Cu tape, optimized to be conductive also from the adhesive side, was considered. In this case, the thin adhesive layer did not affect the electrical contact between polymer and collector and a satisfying metal deposition could be obtained. Not less important, Cu tape is easy-to-use and allows creating specific and on-demand collector geometries.

Before fixing the samples at the cathode, each sample was masked with an insulating polyvinyl acetate film to selectively electrodeposit Cu only at the parallelepiped extremities. The mask was studied to deposit a surface area of 0.8 cm^2. Anode and cathode were fixed to a U-shaped poly-methyl methacrylate (PMMA) support to guarantee the same anode-to-cathode distance in each deposition test and to ensure parallelism between the two (Figure 1). The distance between the electrodes was set at 2.5 cm. A voltage was applied between anode and cathode by a power supply (DuPR10-1-3 Dynatronix). At the same time, an ionic current in the electrolyte solution occurred, making Cu positive ions move and deposit on negative cathode (3D printed conductive sample in this case). Different settings were explored in order to define the right parameters for the electrodeposition; a nominal current of 50 mA (62.5 $mA \cdot cm^{-2}$ current density in this case) was found to be the minimum value for the present setup to start observing Cu deposition on the sample in a reasonable time (5 minutes). Indeed, the PEGDA insulating matrix is known to swell when in contact with water. Therefore, it was necessary to verify if the immersion in the aqueous electrolyte could permanently damage the conductive samples. Three parallelepiped samples with 4.5 mm nominal width were printed. For each sample, four measures were performed with the aid of a digital microscope (Leica DVM2500): the sample width before immersion and the sample width after 5, 10 and 15 minutes immersion inside the electrolyte. Consequently, starting from the minimum, three different nominal currents (50, 100 and 150 mA) at three different times (5, 10 and 15 minutes) were applied for conductive samples Cu electroplating.

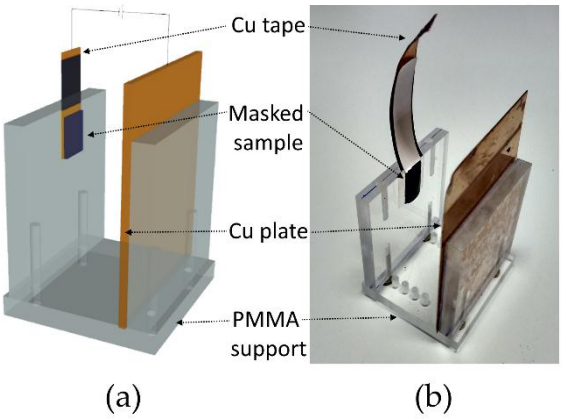

Figure 1 Electrodeposition setup: (a) CAD modeling and (b) actual setup.

A similar masking procedure was employed for the samples deposited with Au sputtering. In this case, an insulating tape was placed on each sample leaving only the extremities exposed to Au deposition. Then, samples were placed into the chamber (Q150T-ES Quorum Technologies) and the pressure was set at 10^{-2} torr. For the deposition process, a 30 mA current for 180 s was selected.

Finally, as regards Ag metallization, conductive Ag paste (RS Pro Silver conducting paste) was manually spread at the samples extremities, covering both the top and three sides of the samples, with a covered surface area similar to the unmasked one for electrodeposited and sputtered samples.

II.VI Electrical and material characterization

Samples were tested before and after metal plating and the electrical characterization was performed using a potentio-dynamic current/voltage (I/V) instrument (Keithley 6430 Cleveland, OH). Tests were carried out measuring 11 current values by applying a voltage from -1 V to +1 V at the samples extremities with two golden probes; mean resistance was calculated and finally conductivity values (σ) were obtained following the relationship reported in (1)

$$\sigma = \frac{l}{R \cdot A} \quad (1)$$

where R is the mean resistance, l the sample length and A the sample section in mm^2. Standard deviation of the obtained values was considered for error estimation.

Moreover, a morphology and atomic composition characterization of the electrodeposited Cu was performed by field emission scanning electron microscopy (FESEM) and energy dispersive X-ray spectroscopy (EDX). For this study, only electrodeposited samples were observed to evaluate the actual morphology of the deposited metal, which was strongly dependent on the presented experimental setup.

III. RESULTS

In this section, results from metal plating with Ag, Au and Cu are reported.

III.I Cu electroplating

Before showing Cu electrodeposition results, it is worth mentioning strength tests performed to assess sample behavior inside the aqueous electrolyte. As reported in Figure 2, a 10% swelling ratio of conductive samples with respect to initial value was observed after 15 min immersion. This deformation was recovered after samples drying without displaying damages.

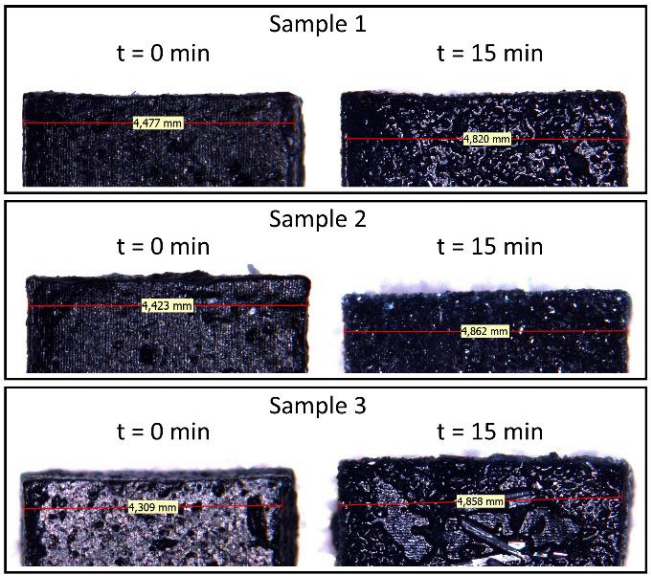

Figure 2 Swelling tests in electroplating electrolyte solution.

Once electroplating maximum process time was chosen in accordance to samples behavior inside the electrolyte solution, Cu was deposited, and samples were tested. The aim was to observe if a conductivity enhancement was achieved. In such case, a higher measured conductivity would not mean a higher bulk material conductivity, but an improved electrical contact between the object and the probes. Electrical characterization results for samples deposited at 50 mA and 100 mA nominal current (62.5 and 125 mA·cm^{-2} respectively) are shown in Figure 3a. Samples subjected to 50 mA nominal current revealed first an increase of electrical conductivity until 10 min treatment and then an unexpected slight decrease with higher process times, with large error bars for all the three analyzed cases. The latter were due to an uneven surface metallization and to a significant qualitative difference in the metal coating from one sample to another (for the same process time and current).

On the other side, samples deposited with 100 mA nominal current showed an increase in the electrical conductivity with higher process times. In this case, it was possible to appreciate the formation of a more uniform Cu film on the 3D printed parts. For lower deposition times, the film was not finely formed, leading to a large error bar and a not-repeatable process. Moving to 10 or 15 minutes deposition, it was possible to observe a better Cu film formation. In particular, for 15 minutes treatment (corresponding to a total charge of 25 mAh and a 10 μm thick Cu layer), it was possible to reach the highest value of electrical conductivity obtained for electroplating Cu deposition (0.15 S·cm^{-1}, one order of magnitude higher than undeposited sample conductivity equal to 0.02 S·cm^{-1}) with an appreciable repeatability.

A further increase to 150 mA nominal current (187.5 mA·cm^{-2}) was detrimental to 3D printed samples, which started cracking during metallization. Thus, no electrical characterization was performed.

A FESEM characterization of the porous electrodeposited Cu layer revealed the presence of the typical Cu grains on the samples deposited with the optimized parameters (100 mA nominal current for 15 min), as visible from Figure 3b. No presence of Cu was observed on the masked regions (Figure 3c).

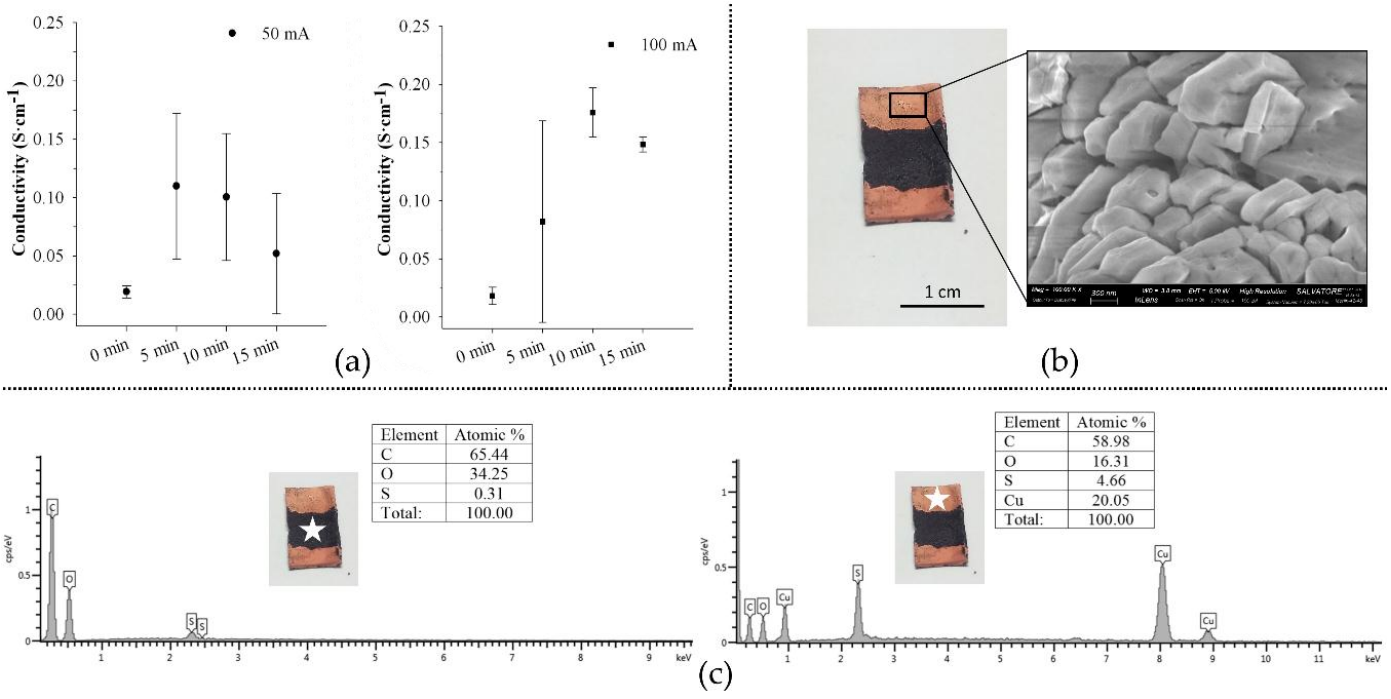

Figure 3 Characterization of 3D printed Cu electroplated PEGDA/PEDOT samples. (a) Electrical characterization results for samples deposited with Cu electrodeposition at 50 mA and 100 mA. (b) A sample electroplated (left) with the optimized parameters (100 mA nominal current for 15 min) and a FESEM image showing the typical Cu grains. (c) Atomic composition of

the "naked" surface (left) and the metal plated surface (right).

III.II Au sputtering and Ag paste

Differently from Cu electroplating, Au sputtering and Ag spreading did not require any optimization for this specific case. Thus, after deposition, electrical characterization was performed and a mean conductivity of 0.03 $S \cdot cm^{-1}$ and 0.16 $S \cdot cm^{-1}$ for Au sputtered and Ag plated parts respectively was found.

IV. DISCUSSION

IV.I Comparison between different metal plating techniques

It is interesting to observe that Ag paste allowed the samples to reach the same increase in electrical conductivity as the Cu electrodeposition method derived from the process at 100 mA nominal current for 15 minutes. Unfortunately, a significant variability was observed (high standard deviation as visible from Figure 4a), but surely it is attributable to the low repeatable manual paste spreading process and the uncontrolled deposited layer thickness (in the order of microns). In contrast, Au sputtering slightly increased the electrical conductivity if compared to the non-metalized polymer, but the measured conductivity was still low with respect to Ag or Cu coated samples. This is probably due to the deposition strategy: Ag paste and Cu were deposited both on the unmasked superior side and lateral side of the parallelepipeds. Instead, Au sputtering, which is a directional process, allows to deposit a metal layer (less than 1 µm thick) only on the upper sample surface orthogonal to the atoms flow inside the sputtering apparatus. Thus, not all the 3D printed layers were connected to the Au layer and probably, during electrical characterization, current couldn't flow homogeneously through the PEGDA/PEDOT sample but only through the upper, or external, surfaces of the body. On the contrary, samples plated with Ag and Cu had a continuous metal coating at their extremities, which allowed to establish a more uniform electrons flow along the sample sections, maximizing the percolative path density due to PEDOT particles in PEGDA matrix. This difference is schematically explained in Figure 4c.

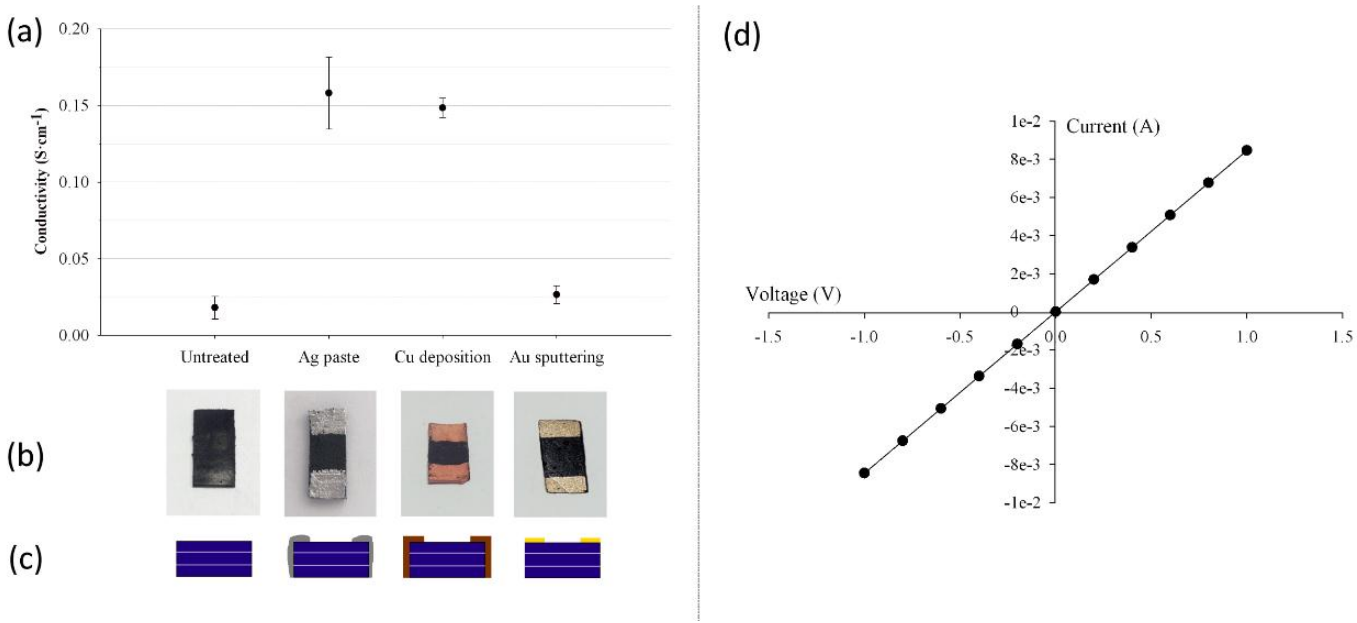

Figure 4 Characterization of plated and un-plated samples (a) Electrical characterization results for samples untreated and treated with Ag paste spreading (Ag paste), Cu electrodeposition (Cu deposition) and Au sputtering (Au sputtering). (b) Samples as they appear after treatment. (c) Schematic image of the samples sections highlighting the differences between the metal plating techniques. (d) I/V plot for the Cu electroplated sample with the optimized parameters; this plot is typical for all the metal plated samples here presented.

Results obtained during electrical characterization revealed also that all the proposed metals are suitable for ohmic contact formation, as visible from the typical I/V plot obtained during testing (Figure 4d), and comparing the different metal plating techniques (Figure 4a), Cu electroplating demonstrated to be the best solution in terms of repeatability and quality of the electrical contact.

Cu electroplating demonstrated to be the best solution also from an economic point of view. Considering process costs referred to the final thickness obtained, Cu electrodeposition and Ag paste deposition involve lower manufacturing costs if compared to sputtering. For sure, sputtering allows for uniform layers deposition with high precision on the final thickness, but the deposited film thicknesses are in the nanometric scale and process cost significantly increases if

layers of the order of the micron-scale are required. Instead, electroplating process allows to reach higher deposited thicknesses, which are controllable as much as applied potential, current density, pH and temperature [39] are tuned. In this case, recursive costs are mainly related to the liquid electrolyte. Nonetheless, the Cu layer is deposited only on unmasked sample areas, thus limiting the associated consumption. Finally, Ag conductive paste allows to create a coarse metal conductive layer without specific equipment, with a low cost per thickness ratio, but with no control on the final thickness. Moreover, Ag paste layer can detach if in contact with water and is supposed to last for a short time. Indeed, the Ag paste can be degraded by PEDOT itself, whose hygroscopic and acidic nature promotes a fast absorption of ambient water corroding the Ag interface [40].

A further consideration can be made concerning samples masking, which is also strictly related to process repeatability. For Ag paste spreading no masking or very simple masking are required, depending on the operator. For sputtering, it is sufficient to control the mask thickness, few tens of microns are compatible to avoid unwanted shadow effects. On the contrary, Cu electroplating requires the material employed for masking to be resistant to acid electrolyte, enough adhesive to ensure a proper coverage during the whole process in aqueous solution (otherwise Cu could deposit infiltrating the detached mask) and, at the same time, easy to remove without sample damage. For sure, masking can represent an issue in Cu electroplating but, if accurately implemented, reproducible results are guaranteed. Table I summarizes the reported considerations.

Table I Comparison between the different metal plating techniques. ✓ indicates advantages, × indicates disadvantages

	Ag paste deposition	**Cu electrodeposition**	**Au sputtering**
Contact enhancement	✓	✓	×
Metal layer thickness	✓	✓	×
Process cost	✓	✓	×
Equipment required	×	✓	✓
Masking precision & repeatability	×	✓	✓
PEDOT compatibility	×	✓	✓

IV.II PEGDA:PEDOT resin: an application

Analyzing the results from the different metal plating techniques, it was interesting to observe that Ag paste allowed the samples to reach the same increase in electrical conductivity as the Cu electrodeposition, but at the cost of a lower repeatability. In contrast, Au sputtering slightly increased the electrical conductivity if compared to the non-metalized polymer, but the measured conductivity was still low with respect to Ag or Cu coated samples. Comparing the different metal plating techniques, Cu electroplating demonstrated to be the best solution in terms of cost effectiveness, repeatability and quality of the electrical contact, combining advantages of Ag paste and sputtered Au.

The active material PEDOT, employed to confer high conductivity to the resin, is of big interest for researchers working with transistors [41], especially the ones based on electrochemical effect [42,43]. Indeed, PEDOT, which is a holes conductor, is able to dope and de-dope when exposed to ionic solutions, thus returning a current signal if properly excited. A preliminary analysis demonstrated that the 3D printed objects maintain the transistor behavior: it was possible to contact the parallelepiped samples on the metalized ends and perform a simple transistor characterization by an electrolyte (NaCl aqueous solution) and an external gate. The transfer characteristic curve of the 3D object was obtained and, as previously stated, a typical electrochemical transistor behavior was observed. The transfer characteristic curve was retrieved applying a constant -0.5 V drain voltage and sweeping the gate voltage (V_{GS}) from -0.75 V to 1 V (Fig. 5). The drain current (I_{DS}) is zeroed as soon as the gate voltage becomes positive, thus inducing electrolyte ions diffusion inside the sample and exhibiting a typical PEDOT based transistors behavior.

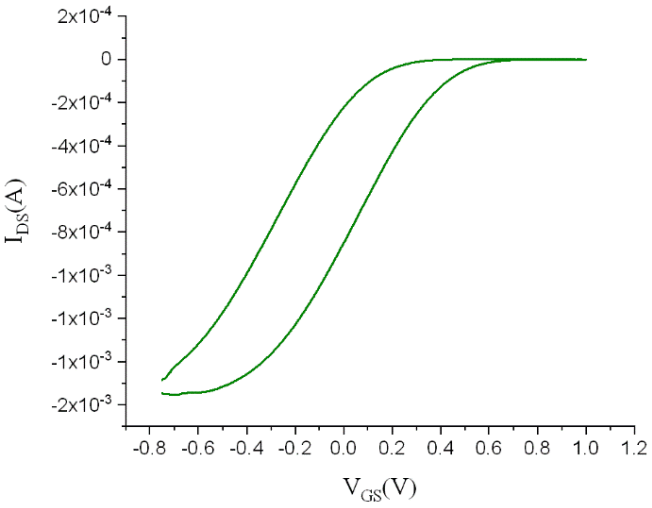

Figure 5 Transfer curve obtained by the 3D object characterization.

As expected, as soon as a negative gate voltage was applied, the transistor changed its conductivity, thus making the effect of an ionic current detectable by a common multimeter (a Keysight B2912A Source/Measure unit). Printable parts with active materials, especially if working at low voltages [44], pave the way for an easy development of wearable devices for health monitoring or smart objects for the Internet of Thing (IoT). In this view, the possibility to effectively integrate

contacts in a 3D printed sensor inside an electronic circuit plays a key role for the design and fabrication of novel customized devices.

Next steps should be dedicated to find a more precise masking technique for electroplating to furtherly promote the process repeatability, as well as the introduction of a different metal. Especially for biomedical applications, the electroplating of gold would reduce possible adverse reactions from skin in case of wearable devices.

V. CONCLUSIONS

In this work, a fast and easy method to metallize the surface of a stereolithography 3D printed electrically conductive polymer composite based on PEDOT:PSS is reported. Ag conductive paste, Cu electroplating and Au sputtering were investigated for understanding pros and cons of each one. The most important effect is the increasing in samples electrical conductivity, thus the establishment of a good electrical contact. Therefore, reaching an effective electrical connection of SL printed PEGDA:PEDOT parts with other electronic elements was the goal of the present study. The driving force lies in a promising application of such additive manufacturing material: fabrication of electrochemical sensors for biomedical purposes.

Conflicts of Interest: The authors declare no conflict of interest.

Funding: The present work was performed in the framework and financed by POLITO BIOMed LAB, DEFLeCT ("Advanced platform for the early detection of not small cells lung cancer") project, financed by Piedmont Region in the framework of "Health &WellBeing" Platform project, and Project "FOOD-DRUG-FREE", financed by Piedmont Region in the framework of "Piedmont BioEconomy Technological Platform" and SMART3D ("Smart 3D Polymer Devices Production Chain") project, financed by MIUR and Piedmont Region agreement in the framework of "Smart Industry".

REFERENCES

[1] C. Weller, R. Kleer, F. T. Piller, *Int. J. Prod. Econ.* **2015**, *164*, 43.

[2] H. Bikas, P. Stavropoulos, G. Chryssolouris, *Int. J. Adv. Manuf. Technol.* **2016**, *83*, 389.

[3] P. F. Jacobs, in *Solid Free. Fabr. Proc.*, **1992**, pp. 196–211.

[4] M. Rong, M. Zhang, H. Liu, H. Zeng, *Polymer (Guildf).* **1999**, *40*, 6169.

[5] E. Fantino, A. Chiappone, F. Calignano, M. Fontana, F. Pirri, I. Roppolo, *Mater. (Basel, Switzerland)* **2016**, *9*, DOI 10.3390/ma9070589.

[6] L. Hu, M. Pasta, F. La Mantia, L. Cui, S. Jeong, H. D. Deshazer, J. W. Choi, S. M. Han, Y. Cui, *Nano Lett.* **2010**, *10*, 708.

[7] M. Mohl, A. Dombovari, R. Vajtai, P. M. Ajayan, K. Kordas, *Sci. Rep.* **2015**, *5*, 13710.

[8] M.-W. Wang, T.-Y. Liu, D.-C. Pang, J.-C. Hung, C.-C. Tseng, *Surf. Coatings Technol.* **2014**, *259*, 340.

[9] S. Kapoor, M. Goyal, P. Jindal, *Indian J. Sci. Technol.* **2017**, *10*, 1.

[10] G. Gonzalez, A. Chiappone, I. Roppolo, E. Fantino, V. Bertana, F. Perrucci, L. Scaltrito, F. Pirri, M. Sangermano, *Polymer (Guildf).* **2017**, *109*, 246.

[11] Y. Liu, W. Xiong, L. J. Jiang, Y. S. Zhou, Y. F. Lu, in (Eds.: B. Gu, H. Helvajian, A. Piqué), **2016**, p. 973808.

[12] E. García-Tuñon, S. Barg, J. Franco, R. Bell, S. Eslava, E. D'Elia, R. C. Maher, F. Guitian, E. Saiz, *Adv. Mater.* **2015**, *27*, 1688.

[13] X. Wei, D. Li, W. Jiang, Z. Gu, X. Wang, Z. Zhang, Z. Sun, *Sci. Rep.* **2015**, *5*, 11181.

[14] B. Román-Manso, F. M. Figueiredo, B. Achiaga, R. Barea, D. Pérez-Coll, A. Morelos-Gómez, M. Terrones, M. I. Osendi, M. Belmonte, P. Miranzo, *Carbon N. Y.* **2016**, *100*, 318.

[15] S. Ummartyotin, J. Juntaro, C. Wu, M. Sain, H. Manuspiya, *J. Nanomater.* **2011**, *2011*, 1.

[16] H. Sirringhaus, T. Kawase, R. H. Friend, T. Shimoda, M. Inbasekaran, W. Wu, E. P. Woo, *Science (80-.).* **2000**, *290*, 2123.

[17] M. A. Saleh, R. Kempers, G. W. Melenka, *Smart Mater. Struct.* **2019**, *28*, 105041.

[18] M. F. Farooqui, M. A. Karimi, K. N. Salama, A. Shamim, *Adv. Mater. Technol.* **2017**, *2*, 1700051.

[19] P. Wei, H. Leng, Q. Chen, R. C. Advincula, E. B. Pentzer, *ACS Appl. Polym. Mater.* **2019**, *1*, 885.

[20] H. Kim, B. R. Wilburn, E. Castro, C. A. Garcia Rosales, L. A. Chavez, T.-L. B. Tseng, Y. Lin, *J. Compos. Mater.* **2019**, *53*, 1319.

[21] S. L. Marasso, M. Cocuzza, V. Bertana, F. Perrucci, A. Tommasi, S. Ferrero, L. Scaltrito, C. F. Pirri, *Rapid Prototyp. J.* **2018**, 00.

[22] E. Suaste-Gómez, G. Rodríguez-Roldán, H. Reyes-Cruz, O. Terán-Jiménez, *Sensors* **2016**, *16*, 332.

[23] M. O. F. Emon, F. Alkadi, D. G. Philip, D.-H. Kim, K.-C. Lee, J.-W. Choi, *Addit. Manuf.* **2019**, *28*, 629.

[24] Y. Gao, G. Yu, T. Shu, Y. Chen, W. Yang, Y. Liu, J. Long, W. Xiong, F. Xuan, *Adv. Mater. Technol.* **2019**, 1900504.

[25] J. R. Windmiller, J. Wang, *Electroanalysis* **2013**, *25*, 29.

[26] Y. Xu, H. Sun, Y. Y. Noh, *IEEE Trans. Electron Devices* **2017**, *64*, 1932.

[27] S. J. Leigh, R. J. Bradley, C. P. Purssell, D. R. Billson, D. A. Hutchins, *PLoS One* **2012**, *7*, 1.

[28] G. Scordo, V. Bertana, L. Scaltrito, S. Ferrero, M. Cocuzza, S. L. Marasso, S. Romano, R. Sesana, F.

Catania, C. F. Pirri, *Mater. Today Commun.* **2019**, *19*, 12.

[29] D. Gentili, P. D'Angelo, F. Militano, R. Mazzei, T. Poerio, M. Brucale, G. Tarabella, S. Bonetti, S. L. Marasso, M. Cocuzza, L. Giorno, S. Iannotta, M. Cavallini, *J. Mater. Chem. B* **2018**, *6*, 5400.

[30] G. Tarabella, A. G. Balducci, N. Coppedè, S. Marasso, P. D'Angelo, S. Barbieri, M. Cocuzza, P. Colombo, F. Sonvico, R. Mosca, S. Iannotta, *Biochim. Biophys. Acta - Gen. Subj.* **2013**, *1830*, 4374.

[31] G. Tarabella, S. L. Marasso, V. Bertana, D. Vurro, P. D'Angelo, S. Iannotta, M. Cocuzza, *Materials (Basel).* **2019**, *12*, 1357.

[32] S. L. Marasso, P. Rivolo, R. Giardi, D. Mombello, A. Gigot, M. Serrapede, S. Benetto, A. Enrico, M. Cocuzza, E. Tresso, C. F. Pirri, *Mater. Res. Express* **2016**, *3*, 065001.

[33] P. D'Angelo, G. Tarabella, A. Romeo, A. Giodice, S. Marasso, M. Cocuzza, F. Ravanetti, A. Cacchioli, P. G. Petronini, S. Iannotta, *MRS Commun.* **2017**, *7*, 229.

[34] S. Stříteský, A. Marková, J. Víteček, E. Šafaříková, M. Hrabal, L. Kubáč, L. Kubala, M. Weiter, M. Vala, *J. Biomed. Mater. Res. Part A* **2018**, *106*, 1121.

[35] A. Elschner, S. Kirchmeyer, W. Lovenich, U. Merker, K. Reuter, *PEDOT*, CRC Press, **2010**.

[36] S. Braun, W. R. Salaneck, M. Fahlman, *Adv. Mater.* **2009**, *21*, 1450.

[37] K. Angel, H. H. Tsang, S. S. Bedair, G. L. Smith, N. Lazarus, *Addit. Manuf.* **2018**, *20*, 164.

[38] N. Saleh, N. Hopkinson, R. J. M. Hague, S. Wise, *Rapid Prototyp. J.* **2004**, *10*, 305.

[39] H. Natter, R. Hempelmann, *J. Phys. Chem.* **1996**, *100*, 19525.

[40] Y. Suh, N. Lu, S. H. Lee, W.-S. Chung, K. Kim, B. Kim, M. J. Ko, M. J. Kim, *ACS Appl. Mater. Interfaces* **2012**, *4*, 5118.

[41] S. Kirchmeyer, K. Reuter, *J. Mater. Chem.* **2005**, *15*, 2077.

[42] V. Preziosi, M. Barra, A. Perazzo, G. Tarabella, R. Agostino, S. L. Marasso, P. D'Angelo, S. Iannotta, A. Cassinese, S. Guido, *J. Mater. Chem. C* **2017**, *5*, 2056.

[43] P. D'Angelo, S. L. Marasso, A. Verna, A. Ballesio, M. Parmeggiani, A. Sanginario, G. Tarabella, D. Demarchi, C. F. Pirri, M. Cocuzza, S. Iannotta, *Small* **2019**, *1902332*, 1902332.

[44] J. Rivnay, S. Inal, A. Salleo, R. M. Owens, M. Berggren, G. G. Malliaras, *Nat. Rev. Mater.* **2018**, *3*, DOI 10.1038/natrevmats.2017.86.